The influence of neuron shape changes on the firing characteristics

Seiichi Sakatani [a] Akira Hirose [a]

[a] *Department of Frontier Informatics, Graduate School of Frontier Sciences, The University of Tokyo, 7-3-1 Hongo, Bunkyo-ku, Tokyo 113-8656, Japan. E-mail: sakatani@eis.t.u-tokyo.ac.jp.*

Abstract

The neuron is highly full of variety in its shape and size. Each neuron has changed its shape to adapt to the region and function in the nervous system. The influence of neuron shape on the firing characteristics, however, has still been unclear. In this paper, we evaluate numerically the influence of the changes of the neuron shape on the firing characteristics. We construct neuronal micro-compartmental models of the pyramidal cell at the CA3 hippocampus to analyze quantitatively the shape dependence of the firing characteristics. We find that, the sharper the shape of the apical-dendrite hillock is, the higher the firing frequency becomes and, at the same time, the firing latency gets shorter for the apical-dendrite synaptic stimulus. These facts lead to a hypothesis that the neuron has changed its shape to respond more sensitively to the stimulus injected at the apical dendrite.

Key words: neuron shape, pyramidal cell, hippocampus, firing rate, firing latency

1 Introduction

The recent progress in physiological measurements has led to new insights into the neuronal behavior. In such efforts, we have recognized the usefulness of neuronal models and constructive methods for analysis by numerical calculation. The authors previously constructed a theory and reported spatiotemporal calculation results of a confluence of membrane potential and its dependence on neuron's configuration[2][4].

The neuron is highly full of variety in its shape and size. In the evolution process, each neuron has changed the shape to adapt to the region and function in the nervous system. Winslow et al.[7] reported that a large part of the variation of whole neuron input resistance is due to variation in the geometry. The authors[2] previously predicted that the signal velocity v on a round soma has a dependence of $v \propto D^{0.77}$ on the conductive-layer thickness D. However, the influence of neuron shape on the firing characteristics has not been investigated in detail.

In this paper, we evaluate numerically the influence of the neuron-shape changes on the firing characteristics. We construct a new neuronal model of the pyramidal cell at the CA3 hippocampus by proposing micro-compartmental models to analyze the firing characteristics quantitatively.

Calculations reveal the following facts: (1)The firing frequency is higher when the shape of the apical-dendrite hillock is sharper. (2)The firing latency is shorter for the apical-dendrite synaptic stimulus when the shape of the apical-dendrite hillock is sharper. These facts lead to a hypothesis that the neuron has changed its shape to respond more sensitively to the stimulus injected at the apical dendrite.

In Section 2, we describe our cell models. Then we show calculation results of the firing rate and firing latency in Section 3. Section 4 gives a discussion. In Section 5, we make our conclusions.

2 Cell model

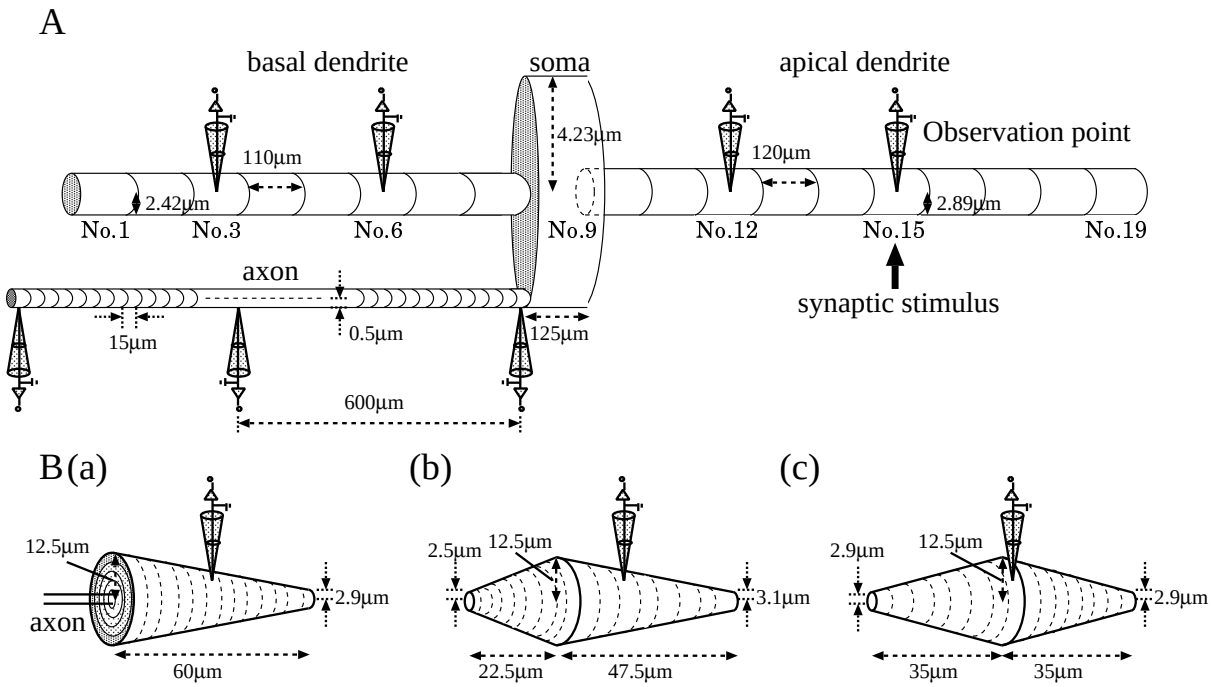

Fig. 1. A. Physical structure of the cell model. Bundled basal dendrites are laid on the left-hand side whereas apical one on the right-hand side. B(a)–(c). Our micro-compartmental soma models instead of the single cylinder. These models have almost the same surface areas. (a)Model B(a). The soma is expressed as a frustum. Radius is 12.5 μm, height is 60 μm. The base area is divided into one circle and four rings. The frustum is divided into 24 cylinders. (b)Model B(b). The soma consists of two frustums. Radii are 12.5 μm, heights are 22.5 and 47.5 μm, respectively. The smaller frustum is divided into 9 cylinders and the bigger one is divided into 19. (c)Model B(c). The soma consists of two symmetrical frustums. Radii are 12.5 μm, heights are 35 μm. Each frustum is divided into 14 cylinders.

We construct our model of a guinea pig CA3 pyramidal cell by placing two types of dendrites, soma, and unmyelinated axon as shown in Fig.1. The basal (left) and apical (right) dendrites in Fig.1 are represented in bundles by equivalent cylinders. In the conventional compartmental model[5], the soma is expressed as one cylinder shown in Fig.1A. The radii (R_k) are 2.42 μm for the basal dendrite, 4.23 μm for the soma, 2.89 μm[5] for the apical dendrite and 0.50 μm[6] for the axon. The lengths of each compartment (H_k) are 110 μm for the basal dendrite, 125 μm for the soma, 120 μm for the apical dendrite and 15 μm for the axon which is small enough to ensure a sufficient stability of calculation for the quick action-potential behavior. (Length constant λ calculated with the parameters described below is 160 μm.) The number of the axon compartments is 80, resulting in a total length of 1200 μm. The basal dendrite cylinder is represented by compartments nos.1–8, the soma by no.9 and the apical dendrite cylinder by compartments nos.10–19, respectively. We call it *Model A* in this paper.

We present our micro-compartmental soma models shown in Figs.1B(a)–(c) and call them *Model B(a)*, *Model B(b)* and *Model B(c)*, respectively. These models have almost the same surface areas. They are divided into cylinders whose heights are 2.5 μm and connected by resistance. In Model B(a), the soma is expressed as a frustum. Base radius is 12.5 μm, top radius is 2.9 μm and height is 60 μm. The base is divided into

one circle and four rings. The frustum is divided into 24 cylinders. In Model B(b), the soma consists of two frustums. Base radii are 12.5 μm, top radii are 2.5, 3.1 μm and heights are 22.5, 47.5 μm, respectively. The smaller frustum is divided into 9 cylinders and the bigger one is into 19. In Model B(c), the soma consists of two symmetrical frustums. Base radii are 12.5 μm, top radii are 2.9 μm and heights are 35 μm. Each frustum is divided into 14 cylinders. We index the somatic compartment nos.S1–S28 or S29. That is, compartment no.9 is now expressed by nos.S1–S28 or S29. Soma no.S1 is connected to the basal dendrite, while soma no.S28 or no.S29 to the apical one.

We determine the passive electric properties of the cell model, such as R_m (membrane resistivity), R_i (intracellular resistivity) and C_m (membrane capacitance), as $R_m = 1.0 \times 10^4$ Ωcm^2 for the soma and dendrites, whereas 1.0×10^3 Ωcm^2 for the axon, $R_i = 1.0 \times 10^2$ Ωcm everywhere, and $C_m = 3$ μF/cm^2 everywhere again.

The dynamics of ionic channel and the distributions of the ionic channel conductance densities are the same as those in Traub et al. (1991) [5], Sakatani and Hirose (2002) [4].

We assume excitatory N-methyl-D-aspartate (NMDA) and α-amino-3-hydroxy-5-methyl-4-isoxazole propionic acid (AMPA) synapses. We use a constant current as NMDA synaptic current for simplicity. The NMDA current is injected into the soma or the apical dendrite 0.66 mm distant from soma (compartment no.15). AMPA synaptic current is injected into the apical dendrite 0.66 mm distant from soma (compartment no.15). The present current waveform equivalent to the AMPA synaptic stimulus is expressed in nA as

$$I_{\mathrm{synaptic}}(t) = G_{\mathrm{syn}}\ t\ e^{-t/\tau}(V - V_{\mathrm{syn}}) \tag{1}$$

where G_{syn} has a unit of mS/s, V is the local membrane potential relative to the resting potential and $V_{\mathrm{syn}} = 60$ mV is the EPSP reversal potential relative to the rest. Time constant $\tau = 2$ ms is consistent with the voltage-clamp data on the mossy fiber EPSP. The full width half maximum (FWHM) pulse width is then about 5 ms.

The conductive-layer thickness is needed for calculation of the current flowing under the soma membrane because the central part of the soma including nucleus is not influenced by the membrane potential gradient. We estimate the effective thickness of the conductive layer D from the intracellular resistance on the condition that the intracellular resistivity is constant. In Model A, intracellular resistance ρ_k is calculated from intracellular resistivity $R_i = 1.0 \times 10^2$ Ωcm, the cylinder-length $H = 1.25 \times 10^2$ μm and the radius $R = 4.23$ μm as

$$\rho_k = R_i H/\pi R^2 = 2.22 \times 10^6 [\Omega] \tag{2}$$

The somatic intracellular resistance in each Model B(a)–(c) is fitted to 2.22 MΩ. The intracellular resistance in Model B(a) $\rho_{\mathrm{B(a)}}$ (in Ω) is expressed as the sum of the resistance at the bottom area and that of the surface area.

$$\rho_{\mathrm{B(a)}} = \sum_{j=S1}^{N_{\mathrm{soma}}} \rho_j = \left\{ \frac{R_i D}{\pi R_{S1}^2} + \sum_{j=S2}^{S5} \frac{R_i}{2\pi D} \log(\frac{R_j}{R_{j-1}}) + \sum_{j=S6}^{S29} \frac{R_i}{\pi D(2\Delta R_j - D)} \Delta H \right\} \times 10^4 \tag{3}$$

Where R_{basal} is the radius of the basal dendrite, R_{soma} is that of the soma, j is the index of the somatic divided cylinder, ΔR_j is the radius of the divided cylinders, ΔH is the height of the divided cylinders, N_{soma} is the number of the soma micro-compartments. The intracellular resistances in Model B(b) and Model B(c)

are expressed as

$$\rho = \sum_{j=S1}^{N_{\mathrm{soma}}} \rho_j = \sum_{j=S1}^{S28} \frac{R_i}{\pi D(2\Delta R_j - D)} \Delta H \times 10^4. \tag{4}$$

As the fitting results with the values calculated by (3) and (4), the effective thicknesses of the conductive layer D in Model B(a)–B are 0.85 μm, 0.87 μm, 0.86 μm, respectively. In the following calculation of the firing characteristics, the time step is 10 ns.

3 Calculation results

In this section, we quantitatively analyze the average firing rate and the firing latency to elucidate the influence of neuron shape changes on the firing characteristics.

3.1 The average firing rate

We calculate the firing frequency when the soma or the distal apical dendrite is stimulated. The CA3 cells express three different modes of firing in response to steady injection of current into the soma, depending on the magnitude of the injected current[8]. The soma generates rhythmic bursts at low frequency for small injected current 0–0.3 nA[1]. At somewhat higher currents 0.3–0.5 nA, rhythmic bursts with intercalated runs of fast spikes occur. At sufficiently large current more than 0.5 nA, rhythmic single action potentials are observed after an initial burst.

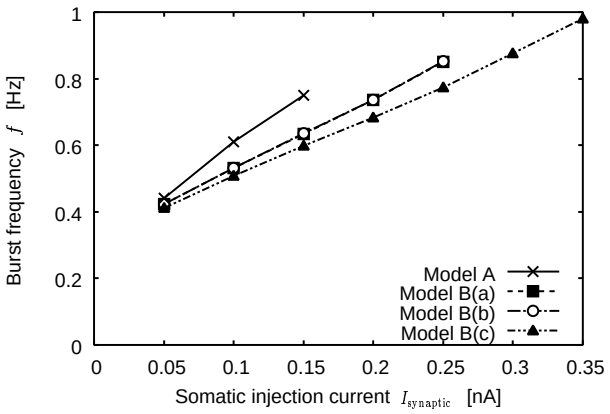

Fig. 2. Frequency-current (f–I_{synaptic}) curves for bursting mode induced by a small somatic current injection.

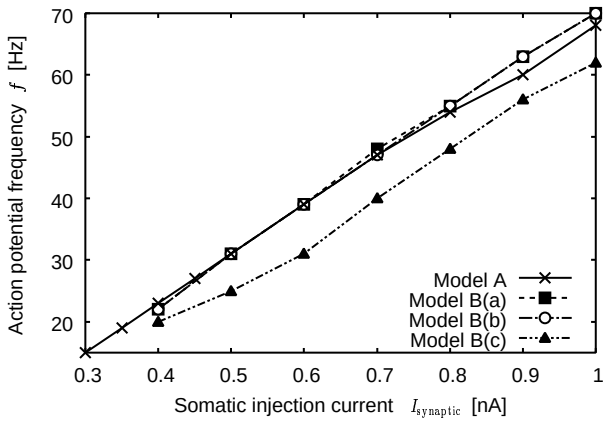

Fig. 3. Frequency-current (f–I_{synaptic}) curves for repetitive action potential mode induced by a large somatic current injection.

Figures 2 and 3 show the relations between the firing frequency f and the somatic injection current I_{synaptic} which mimics the NMDA mediated synaptic stimulus when the soma is stimulated by a constant current. Figure 2 shows the frequency-current curves for the bursting mode induced by a small somatic current injection. In Model A, the burst frequency changes linearly to the injected currents in the range of 0–0.15 nA and the slope is about 3 Hz/nA. At a higher current (larger than 0.2 nA), the rhythmic bursts with intercalated runs of fast spikes occur. In Model B(a), the burst frequency is also proportional to the injected currents of 0–0.25 nA and the slope is about 2 Hz/nA. In Model B(b), the burst frequency also changes linearly to the injected currents of 0–0.25 nA, while the slope is the same as that in Model B(a). In

Model B(c), the burst frequency varies also linearly to the injected currents up to 0.3 nA and the slope is smaller than those in Model B(a) and Model B(b).

Figure 3 shows the frequency-current curves for the repetitive action potential mode induced by the somatic larger current injection. In Model A, the repetitive action potential at 20–70 Hz occurs for the current range of 0.4–1.0 nA. In Model B(a), the repetitive action potential at 22–70 Hz is observed for the current 0.4–1.0 nA. The frequency is the same as that in Model A. The slope is also the same. In Model B(b), the frequency is 22–70 Hz for the current at 0.4–1.0 nA. The curve B(b) is almost the same as that of Model A again. In Model B(c), the frequency is 20–60 Hz for the current at 0.4–1.0 nA. The frequency is smaller than that in Model A.

3.2 The firing latency

In this section, we investigate the temporal evolutions of the membrane potentials at the observation points indicated in Fig.1 when the apical dendrite is stimulated by AMPA synaptic current at 660 μm distant from soma. We report the result of the firing latency. We compare the firing latency in each model on two different conditions. One is for the small synaptic stimulus ($G_{\rm syn} = 0.025$ mS/s) and the other is for the large ($G_{\rm syn} = 0.05$ mS/s). Table 1 shows the comparison of the firing latency when the apical dendrite

Table 1
Comparison of the firing latency when the apical dendrite is synaptically stimulated.

Model	Time[ms] (small stimulus) $G_{\rm syn} = 0.025$ mS/s	Time[ms] (large stimulus) $G_{\rm syn} = 0.05$ mS/s
A	55.6	9.9
B(a)	23.3	9.8
B(b)	23.1	9.8
B(c)	29.9	10.3

(660 μm distant from soma) is stimulated by the synaptic current expressed by (1). For the small stimulus ($G_{\rm syn} = 0.025$ mS/s), the firing latency in Model A is larger than those in others. The firing latencies are identical with those in Model B(a) and Model B(b). That in Model B(c), however, is 6 ms larger when compared with those in Model B(a) and Model B(b). For the large stimulus ($G_{\rm syn} = 0.05$ mS/s), the firing latencies are almost identical with those in all model. The difference of the firing latency is larger when the synaptic stimulus is smaller. In other words, the influence of neuron shape on the firing latency is large when the synaptic stimulus is small.

4 Discussion

The firing characteristics of Model B(a) and Model B(b) are almost the same as those of Model A except the case when the soma is stimulated by a small current injection. The frequencies in Model A is higher than those of Model B(a) and Model B(b). The result of Model B(a) and Model B(b) are good agreement with the experimentally obtained data[8][1] when the soma is stimulated by a small current injection.

We find two significant results. One is the fact that the firing rate in Model B(c) is lower than that of others when the soma is stimulated by the NMDA synaptic current. Pinsky and Rinzel[3] reported the

number of the bursts increases in accordance with the level increase of maximal NMDA conductance so that the NMDA synapses provide a persistent excitation. The NMDA receptor at CA3 has a dominant roll of recalling process in the associative memory. If the pyramidal cell at CA3 change its shape like that in Model B(c), the recalling process may not work appropriately.

The other is that the firing latency in Model B(c) is longer when the apical dendrite is stimulated by the AMPA synaptic current. They[3] also reported that brief stimulation of a single cell in a resting network produces multiple synchronizing population bursts, with fast AMPA synapses providing the dominant synchronizing mechanism. On assumption that all the shapes expressed by Models B(a)–(c) existed at CA3, only those of Model B(c) would not synchronize with others because of their larger latency. For causing the synchronous population bursts, all the pyramidal cells at CA3 choose almost the same shape. Moreover, the actual CA3 cells are in a pyramidal shape, resulting a quick response to the apical stimulus. We can interpret this fact as such that the pyramidal cell at hippocampus CA3 selected its somatic pyramidal shape to respond to the AMPA mediated synaptic stimulus at the apical dendrite more sensitively. This accords with the widely recognized fact that the stimulus fed to the cell at the apical dendrite are the major input signals.

The difference in the frequencies and the latencies are caused by a large resistance gradient on the apical side membrane of Model B(c). If the resistance gradient of a soma is so large as that in Model B(c), the current diffuses from the apical-dendrite hillock to the central part of the soma membrane. For this reason, it takes more time to charge the membrane capacity. Therefore, it takes more time that the membrane potential exceeds its threshold in the nonlinear depolarization dynamics. Therefore, the firing frequency is lower and the firing latency is larger in Model B(c) than those of others.

5 Conclusion

We analyzed the influence of neuron shape on the firing rate and the firing latency. The following two facts have been revealed. First, the firing frequency is higher when the shape of the apical-dendrite hillock is sharper. Secondly, the firing latency is shorter for the apical-dendrite synaptic stimulus when the shape of the apical-dendrite hillock is sharper. These facts lead to a hypothesis that the neuron has changed its shape to respond more sensitively to the stimulus at the apical dendrite.

References

[1] J. J. Hablitz and D. Johnston, "Endogenous nature of spontaneous bursting in hippocampal pyramidal neurons," *Cell. Mol. Neurobiol.*, 1 (1981) 325-334.

[2] A. Hirose, S. Murakami, "Spatiotemporal equations expressing microscopic two-dimensional membrane-potential dynamics," *Neurocomputing*, 43 (2002) 185-196.

[3] P. F. Pinsky and J. Rinzel, "Intrinsic and network rhythmogenesis in a reduced traub model for CA3 neurons," *Journal of computational neuroscience*, 1 (1994) 39-60.

[4] S. Sakatani, A. Hirose, "A quantitative evaluation of the magnetic field generated by a CA3 pyramidal cell at EPSP and action potential," *IEEE Trans. on Biomedical Engineering*, 49 (2002) 310-319.

[5] R. D. Traub, R. K. S. Wong, R. Miles and H. Michelson, "A Model of a CA3 Hippocampal Pyramidal Neuron Incorporating Voltage-Clamp Data on Intrinsic Conductances," *Journal of Neurophysiology*, 66 (1991) 635-650.

[6] R. D. Traub, J. G. R. Jefferys, R. Miles, M. A Whittington and K. Toth, "A branching dendrite model of a rodent CA3 pyramidal neurone," *Journal of Physiology*, 481 (1994) 79-95.

[7] J. L. Winslow, S. E. Jou, S. Wang, J. M. Wojtowicz, "Signals in stochastically generated neurons," *Journal of Computational Neuroscience*, 6 (1999) 5-26.

[8] R. K. S. Wong and D. A. Prince, "Afterpotential generation in hippocampal pyramidal cells," *Journal of Neurophysiology*, 45 (1981) 86-97.